Published in : European Polymer Journal (2021), vol. 152, Article 110453, pp. 1–9
DOI: 10.1016/j.eurpolymj.2021.110453
Status : Postprint (Author's version)

NITROXIDE TEMPO-CONTAINING PILS: KINETICS STUDY AND ELECTROCHEMICAL CHARACTERIZATIONS

Mohamed Aqil [a,b,c,*], Abdelhafid Aqil [a], Farid Ouhib [a], Abdelrahman El Idrissi [b], Mouad Dahbi [c], Christophe Detrembleur [a], Christine Jérôme [a]

[a] *Center for Education and Research on Macromolecules (CERM), University of Liège, B6a Sart–Tilman, B 4000 Liège, Belgium*
[b] *LCAE-URAC 18, Faculty of Science, University of Mohammed Premier, Po Box 717, 60000 Oujda, Morocco*
[c] *Materials Science and Nano-engineering, Mohammed VI Polytechnic University (UM6P), Lot 660 Hay Moulay Rachid, Ben Guerir, Morocco*

Keywords: Cobalt mediated radical polymerization (CMRP), Polymerized ionic liquid (PILs), Redox polymer and organic cathode

Abstract
The cobalt-mediated radical polymerization (CMRP) of new ionic liquid monomers (ILMs), vinyl imidazolium functionalized with redox-active free radical 2,2,6,6-tetramethylpiperidine-1-oxyl (TEMPO)VIm and its CMR copolymerization with vinyl imidazolium units functionalized with triethylene oxide (TEG)VIm produced a well-defined PILs (co)polymers. The controlled nature of (co)polymerization can be seen from the linear first-order kinetic plot, linear evolutions of the molar mass with total monomer conversion and the low polydispersity of the resulting (co)polymers. By combining the redox activity of (TEMPO)PVIm and remarkable ionic conductivity of (TEG)PVIm, outstanding rate capability performance was achieved with a remarkable capacity of 69 mAh g^{-1} at 60C. The obtained organic electrode can serve as sustainable electrodes in lithium ion batteries.

1. Introduction

Polymerized ionic liquid (PILs) attract considerable attention due to their thermal, mechanical and electrochemical properties, for this reason these materials have found potential applications in various fields such as ionic conductive material, porous material and electroactive material to name only a few [1–7]. Among the ionic liquid monomers (ILMs), imidazolium cations remain a popular choice, because they are easy to prepare, present a large variety N-substituent groups and allow the synthesis of different polymers with a wide chemical, as well as their electrochemical stability [8–10]. Moreover, functional imidazolium can be obtained by simple quaternization reaction of vinyl imidazole by bromide derivative [11]. Generally, PILs can be synthesized by postmodification [12] of a neutral polymer precursor, or by free-radical polymerization [1,4,13,14] of ILMs under inert atmosphere. The first method involves the prior preparation of the polymer precursor, introduction of IL moieties generally being carried out by quaternization, however, it's marked by the uncomplete degree of functionalization. The second method results in a large polymer dispersity due to irreversible termination, which will negatively affect the properties of the PILs.

Published in : European Polymer Journal (2021), vol. 152, Article 110453, pp. 1–9
DOI: 10.1016/j.eurpolymj.2021.110453
Status : Postprint (Author's version)

Recently, controlled/living polymerization (CLP) techniques have been used to achieve well-defined PILs with controlled molecular weights, and more importantly, for making copolymers with low dispersity. The CLP of vinyl-imidazolium-type ILMs was investigated using organometallic-mediated radical polymerization (OMRP) [15], the addition − fragmentation chain transfer (RAFT) [16–18], and atom transfer radical polymerization (ATRP) methods [19]. Nevertheless, OMRP and precisely cobalt-mediated radical polymerization (CMRP) remains an efficient way to control homopolymerization and copolymerization of such highly reactive N-vinylimidazolium ionic liquid monomers [20–23].

In our previous work, (TEMPO)VIm was polymerized by free-radical polymerization, before being coated onto a carbon nanotubes buckypaper to be tested as cathode in a lithium ion battery [24]. The obtained battery exhibits a good cycling stability, but with relatively low rate capability 27% of capacity retention at 60 °C. The contribution of the ionic group to the performances of (TEMPO)PVIm is clearly evident compared to a polymer bearing the redox-active TEMPO attached to an acrylate backbone. However, the presence of TEMPO moiety in the imidazolium cation structure decreases the flexibility and the mobility of the cationic polymer backbone, which increase the glass transition temperature (Tg) of the material (Tg = 100 °C) and reduces the ionic mobility. The incorporation of ionic conductor based materials such as (Poly(TEMPO-Substituted Glycidyl ether) [25,26], and poly(TEMPO- substituted methacrylate-co-styrenesulfonate)….) [27–29] has therefore been widely examined to enhance the ionic conductivity of TEMPO- substituted polymer [30,31]. In order to develop a material that can synergistically combine high ionic conductivity and high charge/ discharge capacity, here we report a novel PILs copolymers with TEMPO-substituted imidazolium units and vinyl imidazolium units, functionalized with triethylene oxide substituent. The presence of triethylene oxide pendant groups in imidazolium-based PILs was used to reduce the Tg and to improve their ionic conductivity [1,32,33]. Synthesis of these PILs is carried out in controlled manner under mild experimental conditions using a cobalt-mediated radical polymerization-induced self-assembly (CMRP).

2. Experimental part

2.1. Materials

Bromoacetyl bromide (98% TCI). 4-Hydroxy-2,2,6,6-tetramethylpiperidine 1-oxyl (H-TEMPO) (98% TCI), 2,2,6,6-tetramethylpiperidine- 1-oxy (TEMPO, 98%,Sigma-Aldrich) and all other reagents, including (1-bromoethyl)benzene, 1-Vinylimidazole (99%, Aldrich), Cu^0 powder (75 μm), CuBr, N N,N,N′,N′,N″-pentamethyldiethylenetriamine (PMDETA), bi-pyridine, 2,2′-Azobis(4-methoxy-2.4-dimethyl valeronitrile) (V70) and solvents were purchased from with the highest purity available and used as received without further purification. Lithium bis (trifluoromethanesulfonyl)imide (LiTFSI) (99% ABCR), Sodium bicarbonate ($NaHCO_3$), anhydrous magnesium sulfate ($MgSO_4$), and sodium chloride (NaCl) were of the highest grade, purchased from Sigma-Aldrich, and used without further purification. N,N-Dimethylformamide (DMF), tetrahydrofuran (THF), dichloromethane, ethyl acetate, methanol, toluene, chloroform and diethyl ether were dried using standard procedures, distilled, and stored under argon prior to use. Alkyl-cobalt(III) adduct (R-Co(acac)$_2$) was synthesized and characterized following the previous publications and stored as a stock solution in dichloromethane at −20 °C under argon [34,35]. Electrolyte (1 M LiTFSI in Ethylenecarbonate: Diethylcarbonate: Dimethylcarbonate 1:1:1, EC:DEC:DMC).

Published in : European Polymer Journal (2021), vol. 152, Article 110453, pp. 1–9
DOI: 10.1016/j.eurpolymj.2021.110453
Status : Postprint (Author's version)

2.2. 3-(2-oxo-2-((2,2,6,6-tetramethyl-1-(1-phenylethoxy)piperidin-4-yl) Oxy)ethyl)-1-Vinylimidazolium bromide: (TEMPO)VIm-Br

(TEMPO)VIm-Br was synthesized as described in the previous work [24]. Briefly, 5 g (12.6 mmol) of 2,2,6,6-tetramethyl-1-(1-phenylethoxy) piperidin-4-yl 2-bromoacetate (TEMPO)-Br was slowly added to a solution of 1.77 g (19 mmol) of 1-vinylimidazole in 5 ml of methanol. The mixture was kept under stirring overnight. After concentering the solution, 100 ml ether was added to the mixture, leading to the precipitation of the monomer as a white solid. This solid was then recovered by filtration and purified by recrystallization in acetonitrile. The reaction yield was 5.26 g (85%). ^{1}H NMR (250 MHz, DMSO-d_6) δ 9.54 (s, 1H), 8.28 (s, 1H), 7.90 (s, 1H), 7.43 (dd, J = 15.6, 8.7 Hz, 1H), 7.29 (m, 5H), 6.01 (dd, J = 15.7, 2.5 Hz, 1H), 5.45 (dd, J = 8.8, 2.5 Hz, 1H), 5.29 (s, 2H), 5.00 (m, 1H), 4.74 (q, J = 6.6 Hz, 1H), 1.90 (d, J = 11.9 Hz, 1H), 1.77 (dt, J = 12.6, 3.7 Hz, 1H), 1.54 (dd, J = 22.3, 10.4 Hz, 2H),1.41 (d, J = 6.4 Hz, 3H), 1.30 (s, 3H), 1.18 (s, 3H), 1.03 (s, 3H), 0.60 (s, 3H).

2.3. 1-(2-(2-methoxyethoxy)ethoxy)-2- bromoethane: (TEG-Br)

The bromo compound TEG-Br was synthesized via a modification of literature procedure [33,36,37]. In a typical experiment, triethylene glycol monomethyl ether (2-[2-(2- Methoxy-ethoxy)-ethoxy]-ethanol) (6.4 g, 40 mmol) was added in a well-dried flask containing dry CH_2Cl_2 (160 ml) under an argon atmosphere. Carbon tetrabromide (16 g, 48 mmol) was added to this solution. After cooling the reaction mixture to 0 °C, triphenyl phosphine (16 g, 60 mmol) in dichloromethane (30 ml) was added dropwise to it. After stirring for 6 h, the solvent from reaction mixture was dried under vacuum. 50 ml ether was added to the reaction mixture, which is kept for 5 min before being filtered to get rid of triphenylphospine oxide. The same process (addition of ether, filtration) was repeated thrice. The ether solution was concentrated and was subjected to flash column chromatography (3:1, hexane:ethyl acetate) to obtain the brominated product as a yellow oil. The spectral data for TEG-Br is as follows: ^{1}H NMR (250 MHz, $CDCl_3$, 25 °C, TMS): δ = 3.29 (s, 3H), 3.34 (t, 2H, J = 6 Hz), 3.39 (t, 2H, J = 2.25 Hz), 3.47–3.51 (m, 6H), 3.64 (t, 2H, J = 6 Hz).

2.4. 3-(2-(2-(2-methoxyethoxy)ethoxy)ethyl)-1-vinyl imidazolium bromide: (TEG)VIm-Br

Under stirring, 5 g (18.5 mmol) of (TEG-Br) was slowly added to a solution of 1.9 g (20 mmol) of 1-vinylimidazole in 5 ml of methanol. The mixture was stirred at 80 °C for 24 h. After cooling to room temperature, 100 ml ether was added to the mixture, causing precipitation of the monomer as a yellow oil. The yield was 95%. ^{1}H NMR (300 MHz, DMSO-d_6): δ 3.23 (s, 3H), 3.48 (m, 8H), 3.80 (t, 2H), 4.38 (t, 2H), 5.44 (dd, 1H), 5.97 (dd, 1H), 7.32 (dd, 1H), 7.89 (t, 1H), 8.20 (t, 1H), 9.40 (t, 1H).

2.5. General polymerization procedure

All polymerizations were carried out in DMF with Alkyl Cobalt(III) compound as the initiator in a degassed sealed tube.

2.5.1. Homopolymer (TEMPO)PVIm-Br

The alkyl-Co(III) solution in dichloromethane (0.14 ml, [Co] = 1.38 10^{-1} M, 1.93 × 10^{-2} mmol) was added to a shclenk tube equipped with magnetic stir bar under argon flux, and the solvent was evaporated under vacuum. In another previously prepared schlenk tube, dry DMF (6 ml) was added to 0.5 g of (TEMPO)Vim-Br. The reaction mixture was degassed by five freeze-pumpthaw cycles, until the dissipation of bubbles, filled with argon, and the solution of the

Published in : European Polymer Journal (2021), vol. 152, Article 110453, pp. 1–9
DOI: 10.1016/j.eurpolymj.2021.110453
Status : Postprint (Author's version)

monomer was transferred by the cannula into the first tube containing the alkyl-cobalt(III). The polymerization occurs at 30 °C for five hours and quenched using a degassed DMF-solution of TEMPO. Finally, the crude polymer was purified by precipitation into a large excess of ethanol, the resulting product was dried under vacuum at room temperature (yield: 91%).

2.5.2. Homopolymer (TEG)PVIm-Br

By the same procedure, we synthesized the homopolymer (TEG) PVIm-Br. The polymer obtained was precipitated in ethanol and dried under reduced pressure at room temperature.

2.5.3. Copolymer (TEMPO)PVIm-stat-(TEG)PVIm

The statistical (or random) copolymerization of the two monomers (TEMPO)VIm-Br and (TEG)VIm-Br were preceded by the same procedure. Copolymerization in a single reaction is well established, the ratio of the two monomers have been changed, and as a result, we obtain different polymer composition and characteristics. The residual monomer, $Co(acac)_2$, and excess of TEMPO were removed by dialysis against methanol and dried under vacuum at room temperature overnight, the resulting product was a light green solid.

2.6. Kinetics investigations

For the kinetic study, the polymerization takes place under the same condition and the samples were periodically taken out of the medium via a syringe during the polymerization, the objective was to follow the macromolecular parameters evolution (Mn, Mw/Mn).

2.6.1. Preparation of SEC simples

First, a few drops of TEMPO solution were added to the SEC samples in order to quench the polymerization. Then, after removing the DMF under reduced pressure at 40 °C, 1 ml of a solution of LiTFSI in MeOH (50 mg/ml) was added to each sample and kept under stirring overnight. The polymer was then precipitated in water, centrifuged at 8000 rpm for 10 min. The water was removed and the polymer was washed again with deionized water to remove the residual bromide. The final samples with $TFSI^-$ counter-anion were solubilized in THF/LiTFSI solution (10%wt) and filtered through a nylon membrane filter (0.45 μm).

2.6.2. Preparation of NMR simples

For the determination of the monomer conversion ratio, the ^1H NMR spectrum of the polymerization mixture collected over the polymerization time and quenched by rapid cooling with liquid nitrogen, were measured in DMSO-d_6 at room temperature, and the integration of the monomer $C^-\_C–H$ resonance at around 5.9 ppm was compared with the sum of N-CH-N peak intensity of the imidazolium ring in the polymer and the monomer at around 9.4–9.9 ppm.

Published in : European Polymer Journal (2021), vol. 152, Article 110453, pp. 1–9
DOI: 10.1016/j.eurpolymj.2021.110453
Status : Postprint (Author's version)

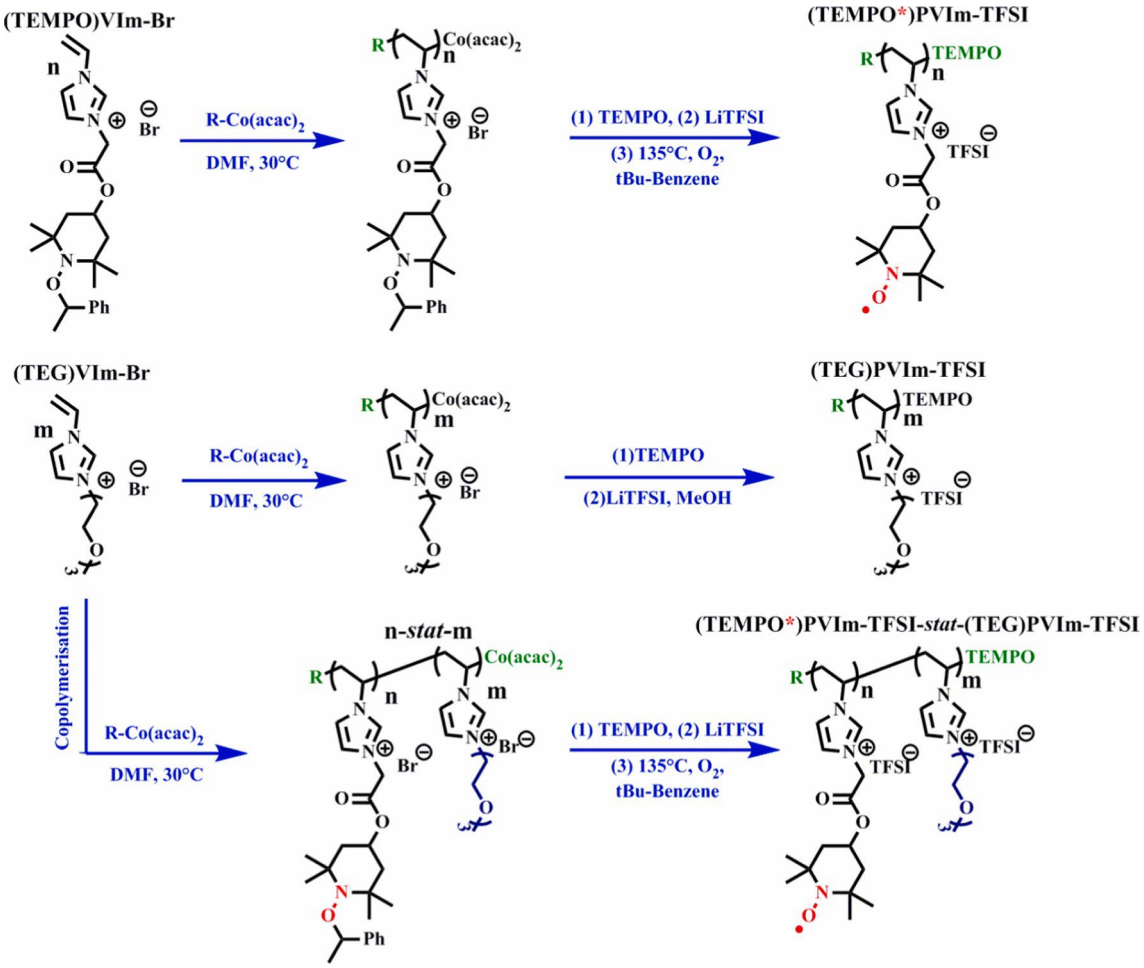

Scheme 1. Synthesis of Pendant TEMPO and TEG containing PILs and statistical copolymers via CMRP of (TEMPO)VIm-Br and (TEG)VIm-Br in DMF at 30 °C, followed by counter-anion exchange and deprotection reaction.

2.7. Typical procedure for the anion exchange reactions to replace bromide by fluorinated anions LiTFSI

The polymers with Br^- counter-anion (2 mmol) was redissolved in methanol and added slowly drop wise to a solution of LiTFSI (2.5 mmol) in MeOH. After one night, the methanol was removed under pressure to provide an oily product in ethyl acetate, which was washed with deionized water five times to remove residual salt (no precipitate of AgBr was observed after testing with AgNO3 solution). After evaporating solvent on a rotary evaporator, the light pink oil was dried under vacuum to yield PILs with $TFSI^-$ counter-anion.

2.8. Oxidation of polymers by thermal treatment

The oxidation was carried out as described previously [38–40], a solution of (TEMPO)PVIm-TFSI or copolymers in *tert*-butylbenzene (C = 0.01 g/ml) were briefly heated at 135 °C in the presence of oxygen for 12 h. The solvent was then removed, and the residue was dissolved in a minimum of dichloromethane and precipitated tree times in diethyl ether before drying in vacuum. The redox PILs was recovered as a dark- brown solid.

Published in : European Polymer Journal (2021), vol. 152, Article 110453, pp. 1–9
DOI: 10.1016/j.eurpolymj.2021.110453
Status : Postprint (Author's version)

2.9. Characterization

^{1}H and ^{13}C NMR spectra of the synthesized material were recorded at 298 K with a Bruker 250 MHz spectrometer using DMSO as solvent. The Fourier transform infrared (FTIR) spectra were recorded with a thermofisher ATR spectrometer instrument using an ATR germanium (Ge) crystal in the range 4000–600 cm^{-1} range. Thermal behavior was determined using a Thermogravimetric Analyzer TGA, Q500 from TA instruments, at a heating rate of 10 °C min^{-1} under a 50 ml min^{-1} nitrogen flow within the range of 25–700 °C.

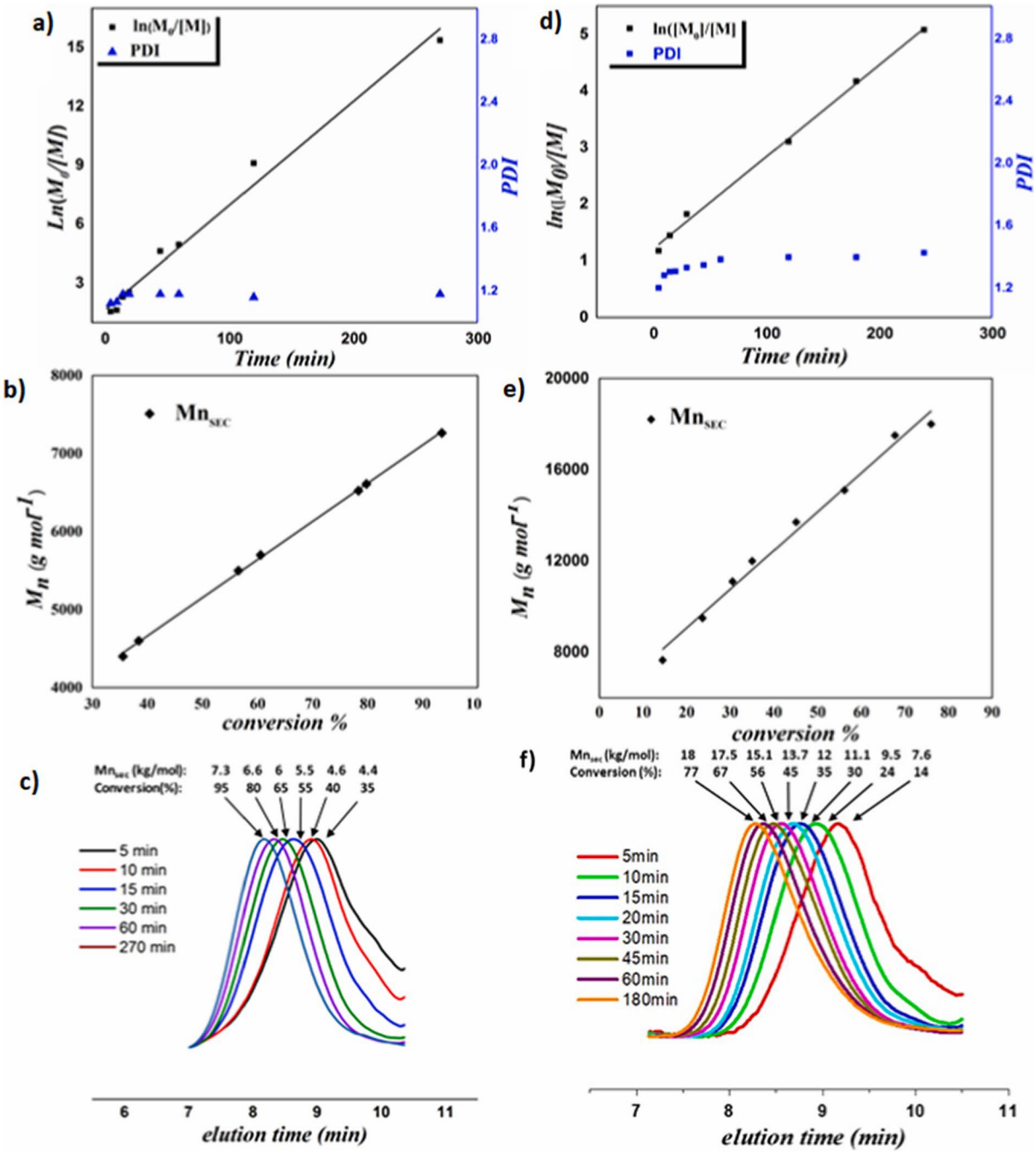

Fig. 1. Semilogarithmic plot with PDI values against polymerization time (a and d), evolution of molar mass of the polymer with the monomer conversion (b and e) and evolution of size exclusion chromatography (SEC) traces (c and f) for the CMRP of (TEMPO)VIm-Br (a, b and c) and statistical copolymer (d, e and f) respectively. The polymerizations initiated by R-Co(acac)$_2$ in DMF at 30 °C. Condition a)*: [(TEMPO)VIm-Br]:[R-Co(acac)$_2$] of 50:1, 1/8:w/v (g/ml)* b)*:[(TEMPO)VIm-Br]: [(TEG) VIm-Br]:[R-Co(acac)$_2$] of 50:50:1, 1/8:w/v (g/ml).*

Published in : European Polymer Journal (2021), vol. 152, Article 110453, pp. 1–9
DOI: 10.1016/j.eurpolymj.2021.110453
Status : Postprint (Author's version)

Differential scanning calorimetric (DSC) analysis was performed on TA DSC Q100 thermal analyzer calibrated with indium, at a heating/cooling rate of 10 °C min^{-1}, under a flowing nitrogen atmosphere with a sample weight of ~10 mg. The glass transition temperature (Tg) was measured at the second heating cycle using TA analysis software provided with the instrument.

The number average molecular weight (Mn) and molecular weight distribution (Mw/Mn) were estimated by size exclusion chromatography (SEC) in tetrahydrofuran (THF) containing 10 mM lithium bis (trifluoromethanesulfonyl)imide (LiTFSI) (flow rate: 1 ml min 1) at 35 ◦C with a SFD S5200 auto sampler liquid chromatograph equipped with an SFD refractometer index detector 2000. PSS SDV analytical linear S 5 µm column (molar mass range: 100–15.105 Da) protected by a PL gel 5 µm guard column and calibrated with poly(styrene) PS standard (580–467,000 g/mol). Omnisec software was used for the treatment of the results.

2.10. Ionic conductivity

PILs in THF solution (2 wt%) was first solvent casted onto an indium tin oxide (ITO) glass substrate and annealed 10 min at 100 °C to remove the solvent. An aluminum electrode was then placed on top of the polymer film. Ionic conductivity σ was measured in the 10–10^6 Hz frequency range, under isothermal conditions, with temperatures ranging from 90 °C to 30 °C and reductions of 10 °C under an inert nitrogen atmosphere. Cell impedance was measured by applying a perturbation of 10 mV in the frequency range of 100 kHz to 1 Hz, at the open circuit potential (OCV). The ohmic resistance (RΩ) of the sample, obtained from the Nyquist plot at the low frequency end of the semicircle, was used to calculate the ionic conductivity using the following equation:

$$\sigma = \frac{l}{A}\frac{1}{R_\Omega}$$

where σ is the conductivity (S/cm), l is the film's thickness (70 nm), A is (the electrode contact surface), RΩ is the resistivity (ohms). Cells were allowed to reach the thermal equilibrium for at least 15 min before each measurement.

2.11. Battery tests

Coin cells (CR2032) were used and assembled in an Ar-filled glove box (MBraun). The PILs/MWNTs composite electrodes were prepared through a dispersing–filtration process [41]: A mixture of MWNTs (5 mg) and PILs (5 mg) was added to acetonitrile (20 ml). The solution was homogenized with an ultrasonic Vibra Cell VCX 750 homogenizer (Sonics & Materials Inc., USA) for 10 min (2 s on, 1 s off), followed by sonication for 2 h at 300 W intensity, and then kept it under steering for 2 more hours. The resulting solution was filtered through a Whatman Anodisc membrane of 0.45 µM pore size, followed by a vacuum drying in a vacuum oven at 80 °C for 12 h to remove the solvent completely before the test. The resulting composite MWNT film was mechanically Robust and was easily removed from the membrane filter. The PILs/MWNT film was directly utilized as the free-standing cathode without any further inclusion of binder, additives, or current collectors. The lithium metal foil was used as an anode. Celgard separator soaked with 100 µl of LP71 (1 M LiTFSI in EC:DEC:DMC 1:1:1) electrolyte was placed between electrodes.

Published in : European Polymer Journal (2021), vol. 152, Article 110453, pp. 1–9
DOI: 10.1016/j.eurpolymj.2021.110453
Status : Postprint (Author's version)

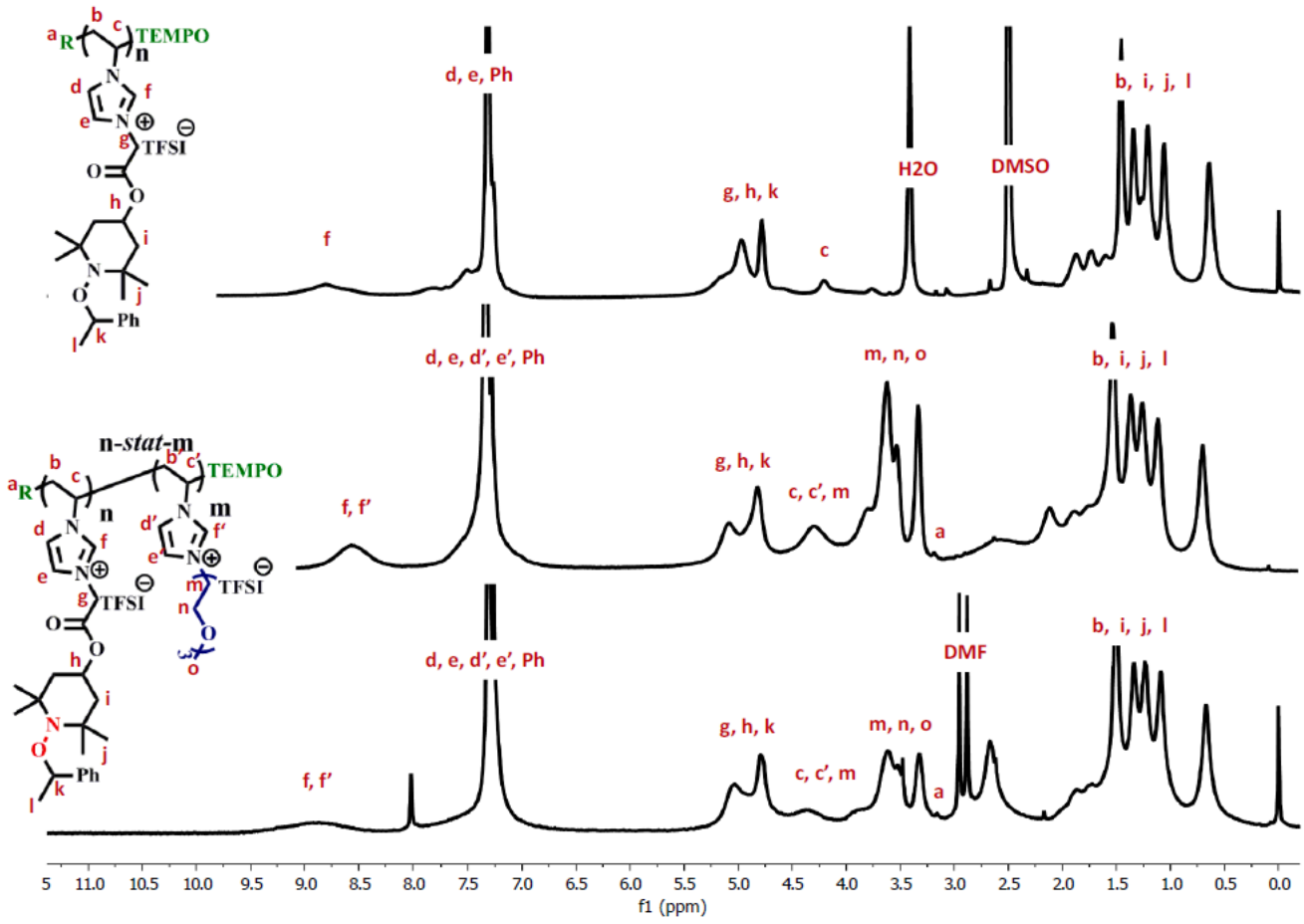

Fig. 2. 1H NMR spectra in DMSO-*d*6 of (TEMPO)PVIm-TFSI, (TEMPO)PVIm40-(TEG)PVIm60 and (TEMPO)PVIm75-(TEG)PVIm25 (up to down respectively).

3. Results and discussion

3.1. Monomers synthesis

The general procedure for the synthesis of (TEMPO)VIm-Br monomer with the protection of the free radical of nitroxide group is well described in our previous reported works [42,43], and the detailed synthetic approach, including experimental conditions and ^{1}H NMR characterization results are given in the Supporting Information (S1–S3).

3.2. Homopolymerization of (TEMPO)VIm-Br and (TEG)VIm-Br

As described in scheme 1, the corresponding homopolymer of (TEMPO)VIm-Br and (TEG)VIm-Br were prepared by CMRP at low temperature (30 °C) in DMF, using alkyl cobalt complex, R-Co(III), as initiator and controlling agent. The alkyl cobalt complex, R-Co(III), showed a very efficient performance to control the polymerization of different monomers, especially N-vinylimidazolium ionic liquid monomers [44–46].

The kinetic study of polymerization reaction of (TEMPO)VIm-Br in DMF at 30 °C with $[Monomer]_0/[alkyl\ cobalt]_0 = 50$ and monomers concentration of 20%wt revealed a linear behavior in the semilogarithmic kinetic plot (Fig. 1a), which

Published in : European Polymer Journal (2021), vol. 152, Article 110453, pp. 1–9
DOI: 10.1016/j.eurpolymj.2021.110453
Status : Postprint (Author's version)

is in agreement with pseudo- first-order kinetic plot, meanwhile, the polydispersity index stays lower to (1.12) at 93% of conversion. This indicates a constant radical concentration throughout the reaction due to the absence of termination processes. Moreover, the molecular weight (Mn_{SEC}) of (TEMPO)PVIm-Br increase in linear manner with the monomer conversion (Fig. 1b), and the SEC traces are monomodal and clearly shift toward higher molecular weight region (Fig. 1c). However, the measured Mn_{SEC} are significantly lower than theoretical values, which could be related to the difference in hydrodynamic volume between (TEMPO)PVIm-TFSI and the linear poly (styrene) (PS) standards used for SEC calibration. Unfortunately, it was not possible to calculate with certitude the experimental number average molecular weight of the polymer from the monomer conversion using ^{1}H NMR spectroscopy, due to the low appearance of the methoxy group characteristic peaks of the alkyl Cobalt initiator. Similarly, we have established conditions for controlled synthesis of (TEG)VIm-Br using alkyl cobalt at 30 °C in DMF $[M]_0/[\text{alkyl cobalt}]_0$ = 100 (Scheme 1). The controlled nature of polymerization can be seen from the linear behavior of the semilogarithmic kinetic plot (figure S4), and also from the linear evolution of Mn_{SEC} with the monomer conversions (figure S5). Low polydispersity was also observed with SEC traces that were unimodal and shifted toward lower elution time with monomer conversion (figure S6).

3.3. Random copolymerization of (TEMPO)VIm-Br and (TEG)VIm-Br

The excellent control nature of the CMRP process has been successfully employed for the preparation of random copolymers. We first investigated the statistical copolymerization with equal molar ratio of monomers, (50/50/1) ([(TEMPO)VIm-Br]/[(TEG)VIm-Br]/[$Co(acac)_2$]) (Scheme 1), using the same operating conditions as described before. Fig. 1d showed the first order kinetics behavior as well as narrow mass distributions. Also, we get the same linear trends in Mn_{SEC} vs monomer conversion (Fig. 1e), and the SEC traces remained monomodal and shifted toward the higher molar mass side with the conversion (Fig. 1f). Likewise, two other copolymers were obtained using two (TEMPO)VIm- Br:(TEG)VIm-Br molar ratios (40:60 and 75:25). Copolymers were finally purified by dialysis against methanol to remove any residual monomer and dried under vacuum. ^{1}H NMR spectra of the copolymers in DMSO-d_6 (Fig. 2) represent the resonance peaks corresponding to both unities in the copolymer and the integrals are in agreement with the theoretical molar ratio. The ratio between the monomers was determined by ^{1}H NMR by comparison of the backbone signal with the peaks of the TEMPO with the integral of the triethyleneoxy group pics.

3.4. Ionic exchange and PILs deprotection

The ATR-FTIR spectra of the PILs are depicted in S7. All compounds show the same characteristic bands of the vinylimidazolium backbone at 2860–2980 cm^{-1} related to the $–CH_3$ and $–CH_2$ stretching vibration of the pendant TEMPO units. IR spectra of ILs and PILs bearing the bis (trifluoromethanesulfonyl)imide ($TFSI^-$) counterion are widely studied in the literature [13,47]. The apparition of new bands in the IR spectrum of (TEMPO)PVIm-TFS, at 1180, 1343 and 1130 cm^{-1} assigned to $\nu_a CF_3$, $\nu_a SO_2$ and $\nu_s SO_2$ respectively can be clearly confirms the successful exchange of the $TFSI^-$ counteranion.

At the final step, the PILs bearing the alkoxyamine C–ON bond was converted into the NO* radical group through a deprotection reaction under aerated condition at 135 °C in *tert*-butylbenzene (scheme 1). As shown in the previous work, at high temperature, the C–ON bond of the alkoxyamine cleaved, releasing TEMPO on the polymer chain while oxygen avoided the back reaction [24]. Figure S8 displays the GPC traces after the deprotection of different copolymers and evidences that, the monomodal signal were remained. *3.5. Thermal behavior and ionic conductivity of PILs*

Published in : European Polymer Journal (2021), vol. 152, Article 110453, pp. 1–9
DOI: 10.1016/j.eurpolymj.2021.110453
Status : Postprint (Author's version)

It's well known that the Imidazolium based PILs Tg's depend sensitively on both the counterion and the grafted group [48]. Generally, exchanging the counterion from Br^- to larger anion, such us $TFSI^-$ influences dramatically the thermal characterization and reduces significantly the Tg's of the PILs [1]. Interestingly, the (TEMPO)PVIm-TFSI homopolymers exhibited a higher Tg's (≈100 °C). An increase in van der Waals interactions between the rigid, bulky TEMPO heterocycle appears to cause this remarkable increase in Tg. it also was found that the presence of more polar group, like carbonyl and nitroxide groups, could contribute to increase the Tg value [49,50]. The (TEG)PVIm-TFSI with

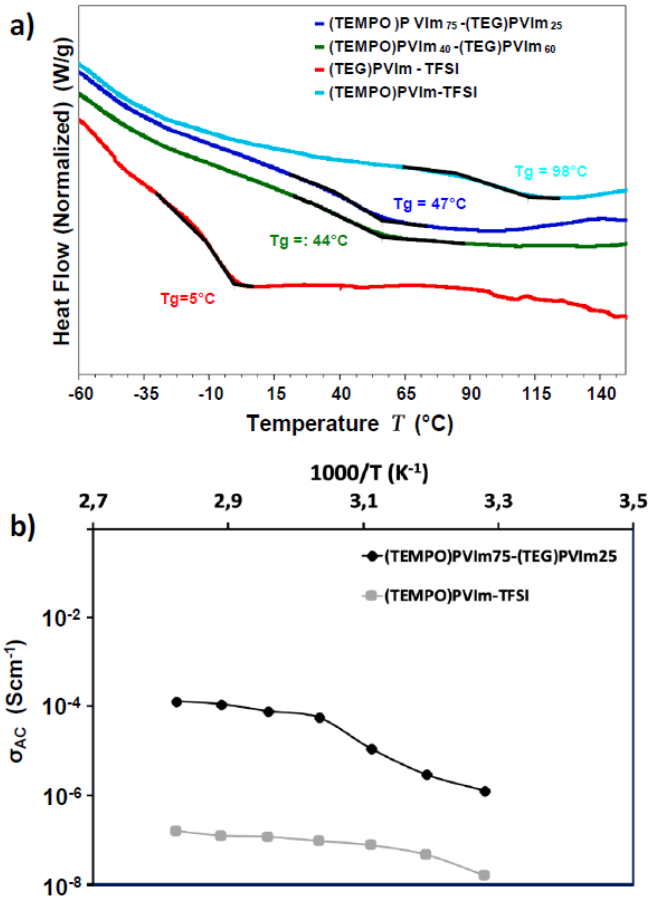

Fig. 3. a: DSC thermograms of (TEMPO)PVIm-TFSI, (TEG)PVIm-TFSI and different copolymers (TEMPO)PVIm-(TEG)PVIm with 25% and 60% of TEG unities under nitrogen atmosphere at 10 °C min^{-1}. b: Temperature dependence of the ionic conductivity for (TEMPO)PVIm-TFSI and (TEMPO)$PVIm_{75}$-(TEG) $PVIm_{25}$ electrolytes.

Table 1
Molecular weights, Tg's and ionic conductivities of synthesized PILs.

PILs	Mn_{SEC}[a] (kg/mol)	Mn_{RMN}[b] (kg/mol)	PDI[a]	Tg (°C)[c]	σ₀ at 30 °C (Scm− 1)[d]
(TEMPO)PVIm-TFSI	7.5	32	1.2	98	$1.59\ 10^{-6}$
(TEG)PVIm-TFSI	12	–	1.3	5	–
(TEMPO)$PVIm_{75}$-(TEG)$PVIm_{25}$	77	110	2.0	47	$1.28\ 10^{-4}$
(TEMPO)$PVIm_{40}$-stat-(TEG) PVIm60	44	94	2.2	44	–

Reported values obtained by:
[a] Mn_{SEC} were estimated by SEC against PS standard.

Published in : European Polymer Journal (2021), vol. 152, Article 110453, pp. 1–9
DOI: 10.1016/j.eurpolymj.2021.110453
Status : Postprint (Author's version)

[b] Mn_{NMR} was calculated in ^1H NMR by comparing the integral of the methoxy group at the chain-end of the alkyl-cobalt initiator (Ha ≈ 3.17 ppm), with that of the TEMPO group of the repeat unit (H_g, H_h and H_k at 4.7–5.7 ppm) and with that of TEG group (H_o at ≈3.7 ppm).

[c] Tg was measured by DSC at the second heating cycle at a rate of 10 °C min^{-1}.

[d] σ was measured in the 10–10^6 Hz frequency range at a temperature ranging from 90 °C to 30 °C.

linear functional group have a lower Tg (≈5 °C), due to their flexible nature caused by the elevated chain mobility of the TEG ether groups, presumably it is facilitated by the electrostatic interactions in the cationic poly(N-vinyl-imidazolium)s based PILs [14,51–54]. The introduction of ethylene oxide pendant groups in (TEMPO)PVIm-TFSI polymer decrease the Tg (Fig. 3a), facilitates mobility of the polymer chains

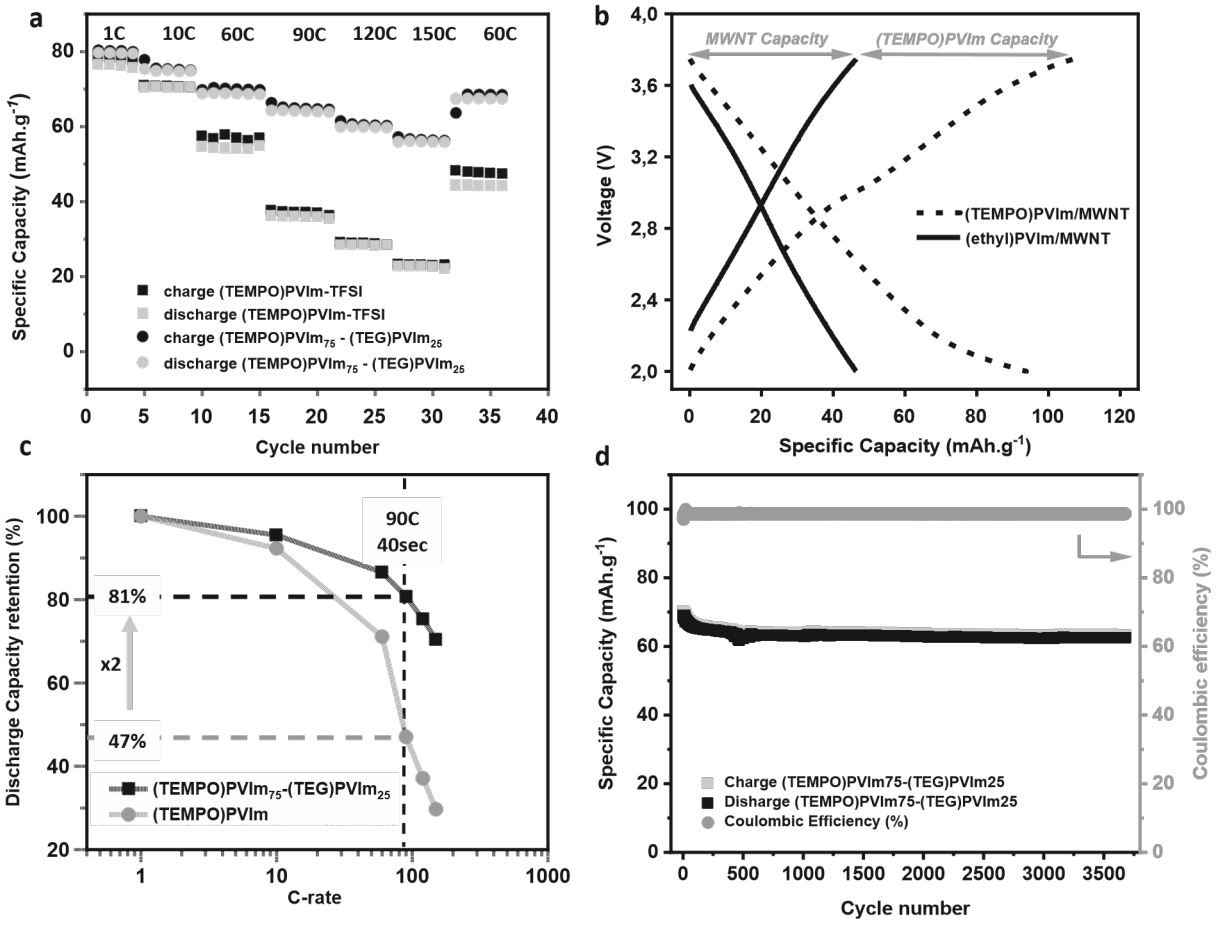

Fig. 4. Comparative electrochemical performance for the (TEMPO)PVIm/MWNTs and (TEMPO)$PVIm_{75}$-(TEG)$PVIm_{25}$/MWNTs buckypaper electrodes in Li-ion half- cells. a: rate capability: discharge capacity vs cycle number, b: charge/discharge voltage profile of the (TEMPO)PVIm/MWNTs and (ethyl)PVIm/MWNTs at a rate of 1C in the potential range from 2 to 3.8 V (Vs Li/Li^+), c: Modified Peukert plots, indicating retention of discharge capacity as a function of C rate in logarithmic scale (Capacity at different C rate are normalized with respect to the capacity at 1C = 45 mA g^{-1}), d: long-term cyclability and coulombic efficiencies measured at 60C.

and thus increases the ionic conductivity. Otherwise, there is not significant decrease in the Tg values between the copolymers with 25% and 60% of TEG unities (Tg ≈ 49 °C and Tg ≈ 44 °C respectively). In order to respect the balance between low Tg/high ionic conductivity combined with the maximum of energy density, we kept only the copolymer with 75–25 M ratio for the electrochemical properties characterizations (see Table 1).

Published in : European Polymer Journal (2021), vol. 152, Article 110453, pp. 1–9
DOI: 10.1016/j.eurpolymj.2021.110453
Status : Postprint (Author's version)

3.6. Ionic conductivity

The temperature dependence of the anhydrous ionic conductivity (σ_{AC}) of (TEMPO)PVIm-TFSI homopolymers and (TEMPO)$PVIm_{75}$- (TEG)$PVIm_{25}$ copolymer were then evaluated by using the electrochemical impedance spectroscopy (EIS) using a thin film of PILs (70 nm). In all case, the ionic conductivity increases with increasing temperature, as is typical of polymer electrolytes (Fig. 3b). There is also a significant effect from the presence of triethyleneoxy (TEG) in the copolymer versus the homopolymer on ionic conductivity. The room temperature ionic conductivity of (TEMPO) $PVIm_{75}$-(TEG)$PVIm_{25}$ ($1.28\ 10^{-4}\ Scm^{-1}$) is almost 100-fold higher than that of the (TEMPO)PVIm- TFSI ($1.59\ 10^{-6}\ Scm^{-1}$). The diethyleneoxy units on the imidazolium cation afford a higher ionic conductivity by decreasing Tg and contributing to the ion pair dissociation, as well as promoting their solubilization and mobility [32].

3.7. Electrochemical characterization

Nitroxide radical based material still one of the most studied polymers in energy storage application, due to its ultra-fast electrochemical response and higher working potential [41–43,55–57]. In order to compare the power performance of the two PILs, half-cells with buckypaper composite electrodes based on PILs-supported TEMPO radicals as working electrode, lithium plate as the counter electrode and LiTFSI as electrolyte were fabricated (S9). The electrochemical power performances were measured by galvanostatic charge/discharge experiments in the potential range from 2 to 3.8 V (Vs Li/Li^+) at different C-rate (1-150C).(Fig. 4a) Note that for a proper comparison of the specific capacities of PILs/MWNT electrodes only the active blocks (TEMPO)PVIm are considered. The capacity of the cathode was calculated based on the total weight of the active polymer (TEMPO)PVIm- TFSI which is determined by TGA analysis (S10). At C-rate of 1C, both PILs show almost the same reversible capacity with a slight difference 80 mAh g^{-1} and 77 mAh g^{-1} for (TEMPO)PVIm-TFSI/MWNTs and (TEMPO)$PVIm_{75}$-(TEG)$PVIm_{25}$/MWNTs respectively, which is 78% higher than the theoretical capacity of homopolymer (45 mAh g^{-1}). To highlight this capacity excess, Fig. 4b shows a comparison of the charge/ discharge voltage profile of the (TEMPO)PVIm/MWNTs and (ethyl) PVIm/MWNTs at a rate of 1C in the potential range from 2 to 3.8 V (Vs Li/Li^+). The composite electrode PILs/MWNTs with the non-redox- active ethyl groups exhibits a discharge capacity of 45 mAh g^{-1} which is attributed to the electric double-layer capacitance (EDLC). This is fully consistent with the previous obtained results [24,45]. The discharge capacities continue to decrease with increase in the current intensity, but with more effect in the case of homopolymer. For 60C (60 s for total discharge), we still get a high reversible capacities of 69 (87%) and 54.5 (71%) mAh g^{-1} for copolymer and the homopolymer respectively. At a higher C-rate (90, 120 and 150C), (TEMPO)$PVIm_{75}$-(TEG)$PVIm_{25}$/ MWNTs still demonstrate an excellent rate performance with discharges capacities of 64.2, 60 and 56 mAh g^{-1}, which is more than two times higher than that of (TEMPO)PVIm-TFSI/MWNTs at the same C-rate (Fig. 4c). When the current rate reverses back to 60C, both cells capacity immediately recovers to its original value. This suggests that the presence of ethylene oxide pendant groups in imidazolium-based PILs improves the material ionic conductivity, which solves the limitations of ion species diffusion responsible for the reduced material activity at higher C-rates. Fig. 4.d demonstrate the long-term cyclability of (TEMPO)$PVIm_{75}$-(TEG)$PVIm_{25}$ /MWNTs electrode material. A very stable capacity retention, 92% of the initial discharge capacity, was obtained after 3600 cycles at 60C with 100% of the coulombic efficiency during the whole cycling test. This high electrochemical performance are assumed to be the results of: (i) the stable and ultra-rapid redox reaction of the nitroxide group, (ii) the high ionic conductivity of the PILs with its negligible solubility into the non-aqueous electrolyte solution, (iii) the excellent electronic conductivity of three dimensional MWNTs network.

4. Conclusion

This contribution reports the well synthesis in a controlled way and with narrow PDIs of a new redox active poly(ionic liquid)s PILs using cobalt mediated radical polymerization at moderate temperatures (30C). (TEMPO)PVIm-TFSI with bis(trifluoromethanesulfonylimide) counterion was obtained through an easy anion exchange reaction and thermal deprotection by oxidative aerobic C–ON bond homolysis. Besides, copolymers of PILs containing not only TEMPO but also triethyleneglycol pendant groups were prepared to improve the ionic conductivity and increase the electrochemical performances with a remarkable capacity of 69 mAh g^{-1} at 60C, and impressively retained 87% of its initial capacity at 1C. The excellent performances (TEMPO) PVIm-(TEG)PVIm copolymer as an organic cathode active material was back to the synergistic effect between high stability of the radical PILs (TEMPO)PVIm-TFSI and high ionic conductivity of the (TEG)PVIm-TFSI.

CRediT authorship contribution statement

Mohamed Aqil: Writing - original draft, Visualization. **Abdelhafid Aqil:** Writing - review & editing. **Farid Ouhib:** Conceptualization. **Abdelrahman El Idrissi:** Supervision. **Mouad Dahbi:** Visualization, Investigation. **Christophe Detrembleur:** Investigation. **Christine Jérôme:** Supervision, Resources.

Appendix A. Supplementary material

Supplementary data to this article can be found online at https://doi.org/10.1016/j.eurpolymj.2021.110453.

References

[1] M.H. Allen, S. Wang, S.T. Hemp, Y. Chen, L.A. Madsen, K.I. Winey, T.E. Long, Hydroxyalkyl-containing imidazolium homopolymers: correlation of structure with conductivity, Macromolecules 46 (2013) 3037–3045, https://doi.org/10.1021/ ma302537f.

[2] K. Nakamura, T. Saiwaki, K. Fukao, T. Inoue, Viscoelastic Behavior of the Polymerized Ionic Liquid Poly(1-ethyl-3-vinylimidazolium bis (trifluoromethanesulfonylimide)), Macromolecules 44 (2011) 7719–7726, https:// doi.org/10.1021/ma201611q.

[3] G. Colliat-Dangus, M.M. Obadia, Y.S. Vygodskii, A. Serghei, A.S. Shaplov, E. Drockenmuller, Unconventional poly(ionic liquid)s combining motionless main chain 1,2,3-triazolium cations and high ionic conductivity, Polym. Chem. 6 (2015) 4299–4308, https://doi.org/10.1039/C5PY00526D.

[4] K. Yin, Z. Zhang, L. Yang, S.-I. Hirano, An imidazolium-based polymerized ionic liquid via novel synthetic strategy as polymer electrolytes for lithium ion batteries, J. Power Sources 258 (2014) 150–154, https://doi.org/10.1016/j. jpowsour.2014.02.057.

[5] I. Osada, H. De Vries, B. Scrosati, S. Passerini, Ionic-liquid-based polymer electrolytes for battery applications, Angew. Chemie - Int. Ed. 55 (2016) 500–513, https://doi.org/10.1002/anie.201504971.

[6] A.S. Shaplov, R. Marcilla, D. Mecerreyes, Recent advances in innovative polymer electrolytes based on poly(ionic liquid)s, Electrochim. Acta 175 (2015) 18–34, https://doi.org/10.1016/J.ELECTACTA.2015.03.038.

[7] J. Yuan, M. Antonietti, Poly(ionic liquid)s: polymers expanding classical property profiles, Polymer (Guildf) 52 (2011) 1469–1482, https://doi.org/10.1016/J. POLYMER.2011.01.043.

[8] D. Mecerreyes, Polymeric ionic liquids: broadening the properties and applications of polyelectrolytes, Prog. Polym. Sci. 36 (2011) 1629–1648, https://doi.org/ 10.1016/j.progpolymsci.2011.05.007.

[9] J. Yuan, D. Mecerreyes, M. Antonietti, Poly(ionic liquid)s: an update, Prog. Polym. Sci. 38 (2013) 1009–1036, https://doi.org/10.1016/j.progpolymsci.2013.04.002.

[10] D.R. MacFarlane, N. Tachikawa, M. Forsyth, J.M. Pringle, P.C. Howlett, G. D. Elliott, J.H. Davis, M. Watanabe, P. Simon, C.A. Angell, Energy applications of ionic liquids, Energy Environ. Sci. 7 (2014) 232–250, https://doi.org/10.1039/ C3EE42099J.

[11] A. Tkacheva, J. Zhang, B. Sun, D. Zhou, G. Wang, A.M. McDonagh, TEMPO-ionic liquids as redox mediators and solvents for Li–O 2 batteries, J. Phys. Chem. C. 124 (2020) 5087–5092, https://doi.org/10.1021/acs.jpcc.0c00367.

[12] B.S. Aitken, C.F. Buitrago, J.D. Heffley, M. Lee, H.W. Gibson, K.I. Winey, K. B. Wagener, Precision ionomers: synthesis and thermal/mechanical characterization, Macromolecules 45 (2012) 681–687, https://doi.org/10.1021/ ma202304s.

[13] K. Grygiel, J.S. Lee, K. Sakaushi, M. Antonietti, J. Yuan, Thiazolium poly(ionic liquid)s: synthesis and application as binder for lithium-ion batteries, ACS Macro Lett. 4 (2015) 1312–1316, https://doi.org/10.1021/acsmacrolett.5b00655.
[14] J.H. Lee, J.S. Lee, J.W. Lee, S.M. Hong, C.M. Koo, Ion transport behavior in polymerized imidazolium ionic liquids incorporating flexible pendant groups, Eur. Polym. J. 49 (2013) 1017–1022, https://doi.org/10.1016/j.eurpolymj.2013.01.026.
[15] D. Cordella, A. Kermagoret, A. Debuigne, C. Jérôme, D. Mecerreyes, M. Isik, D. Taton, C. Detrembleur, All poly(ionic liquid)-based block copolymers by sequential controlled radical copolymerization of vinylimidazolium monomers, Macromolecules 48 (2015) 5230–5243, https://doi.org/10.1021/acs.macromol.5b01013.
[16] H. Mori, M. Yahagi, T. Endo, RAFT polymerization of N -vinylimidazolium salts and synthesis of thermoresponsive ionic liquid block copolymers, Macromolecules 42 (2009) 8082–8092, https://doi.org/10.1021/ma901180j.
[17] B. Zhang, X. Yan, P. Alcouffe, A. Charlot, E. Fleury, J. Bernard, Aqueous RAFT polymerization of imidazolium-type ionic liquid monomers: en route to poly(ionic liquid)-based nanoparticles through RAFT polymerization-induced self-assembly, ACS Macro Lett. 4 (2015) 1008–1011, https://doi.org/10.1021/ acsmacrolett.5b00534.
[18] N. Corrigan, K. Jung, G. Moad, C.J. Hawker, K. Matyjaszewski, C. Boyer, Reversible-deactivation radical polymerization (Controlled/living radical polymerization): From discovery to materials design and applications, Prog. Polym. Sci. 111 (2020), 101311, https://doi.org/10.1016/j.progpolymsci.2020.101311.
[19] A.R.S. Santha Kumar, N.K. Singha, Reversible Addition-Fragmentation Chain Transfer (RAFT) polymerization in ionic liquids: a sustainable process BT - advances in sustainable polymers: synthesis, fabrication and characterization, Springer Singapore, Singapore, 2020, pp. 183–193.
[20] A. Debuigne, C. Jérôme, C. Detrembleur, Organometallic-mediated radical polymerization of 'less activated monomers': fundamentals, challenges and opportunities, Polym. (United Kingdom) 115 (2017) 285–307, https://doi.org/ 10.1016/j.polymer.2017.01.008.
[21] C. Detrembleur, A. Debuigne, M. Hurtgen, J. Christine, J. Pinaud, P. Coupillaud, J. Vignolle, D. Taton, Synthesis of 1-Vinyl-3-ethylimidazolium-based ionic liquid (Co) polymers by cobalt-mediated radical polymerization, Macromolecules (2011) 6397–6404.
[22] C.H. Peng, T.Y. Yang, Y. Zhao, X. Fu, Reversible deactivation radical polymerization mediated by cobalt complexes: recent progress and perspectives, Org. Biomol. Chem. 12 (2014) 8580–8587, https://doi.org/10.1039/c4ob01427h.
[23] J.L. Shamshina, O. Zavgorodnya, R.D. Rogers, Ionic Liquids, in: Ref. Modul. Chem. Mol. Sci. Chem. Eng., Elsevier, 2018. https://doi.org/10.1016/B978-0-12-409547- 2.13931-9.
[24] M. Aqil, F. Ouhib, A. Aqil, A. El Idrissi, C. Detrembleur, C. Jérôme, Polymer ionic liquid bearing radicals as an active material for organic batteries with ultrafast charge-discharge rate, Eur. Polym. J. 106 (2018) 242–248, https://doi.org/ 10.1016/J.EURPOLYMJ.2018.07.028.
[25] K. Sato, T. Sukegawa, K. Oyaizu, H. Nishide, Synthesis of poly(TEMPO-substituted glycidyl ether) by utilizing t-BuOK/18-crown-6 for an organic cathode-active material, Macromol. Symp. 351 (2015) 90–96, https://doi.org/10.1002/ masy.201300224.
[26] T. Sukegawa, K. Sato, K. Oyaizu, H. Nishide, Efficient charge transport of a radical polyether/SWCNT composite electrode for an organic radical battery with high charge-storage density, RSC Adv. 5 (2015) 15448–15452, https://doi.org/ 10.1039/C4RA15949G.
[27] B. Il, S. Chae, M. Koyano, K. Oyaizu, H. Nishide, I.S. Chae, M. Koyano, K. Oyaizu, H. Nishide, Self-doping inspired zwitterionic pendant design of radical polymers toward a rocking-chair-type organic cathode-active material, J. Mater. Chem. A. 1 (2013) 1326, https://doi.org/10.1039/c2ta00785a.
[28] I.S. Chae, M. Koyano, T. Sukegawa, K. Oyaizu, H. Nishide, Redox equilibrium of a zwitterionic radical polymer in a non-aqueous electrolyte as a novel Li+ host material in a Li-ion battery, J. Mater. Chem. A. 1 (2013) 9608, https://doi.org/ 10.1039/c3ta12076g.
[29] H. Tokue, T. Murata, H. Agatsuma, H. Nishide, K. Oyaizu, Charge–discharge with rocking-chair-type Li + Migration characteristics in a zwitterionic radical copolymer composed of TEMPO and trifluoromethanesulfonylimide with carbonate electrolytes for a high-rate Li-Ion battery, Macromolecules 50 (2017) 1950–1958, https://doi.org/10.1021/acs.macromol.6b02404.
[30] J. Hong, J. Seung, J. Lee, S. Man, C. Min, Ion transport behavior in polymerized imidazolium ionic liquids incorporating flexible pendant groups, Eur. Polym. J. 49 (2013) 1017–1022, https://doi.org/10.1016/j.eurpolymj.2013.01.026.
[31] K. Hatakeyama-Sato, T. Tezuka, R. Ichinoi, S. Matsumono, K. Sadakuni, K. Oyaizu, Metal-free, solid-state, paperlike rechargeable batteries consisting of redox-active polyethers, ChemSusChem. (2020) cssc.201903175. https://doi.org/10.1002/cssc. 201903175.
[32] M. Lee, U.H. Choi, R.H. Colby, H.W. Gibson, Ion conduction in imidazolium acrylate ionic liquids and their polymers, Chem. Mater. 22 (2010) 5814–5822, https://doi.org/10.1021/cm101407d.
[33] T.K. Carlisle, E.F. Wiesenauer, G.D. Nicodemus, D.L. Gin, R.D. Noble, Ideal CO_2/ light gas separation performance of poly (vinylimidazolium) membranes and poly (vinylimidazolium) -ionic liquid composite films, Ind. Eng. Chem. Res. 52 (2013) 1023–1032.
[34] D. Cordella, A. Kermagoret, A. Debuigne, R. Riva, I. German, M. Isik, C. Jérôme, D. Mecerreyes, D. Taton, C. Detrembleur, Direct route to well-defined poly(ionic liquid)s by controlled radical polymerization in water, ACS Macro Lett. 3 (2014) 1276–1280, https://doi.org/10.1021/mz500721r.
[35] A. Debuigne, C. Michaux, C. Jérôme, R. Jérôme, R. Poli, C. Detrembleur, Cobalt- mediated radical polymerization of acrylonitrile: kinetics investigations and DFT calculations, Chem. – A Eur. J. 14 (2008) 7623–7637, https://doi.org/10.1002/ chem.200800371.
[36] I. Kim, H. Tsai, K. Nishi, T. Kasagami, B.D. Hammock, NIH public access, NIH Public Access. 50 (2008) 5217–5226, https://doi.org/10.1021/jm070705c.1.

[37] B. Karimi, F. Mansouri, H. Vali, A highly water-dispersible/magnetically separable palladium catalyst based on a Fe3O4@SiO2 anchored TEG-imidazolium ionic liquid for the Suzuki-Miyaura coupling reaction in water, Green Chem. 16 (2014) 2587, https://doi.org/10.1039/c3gc42311e.

[38] F. Behrends, H. Wagner, A. Studer, O. Niehaus, H. Eckert, F. Behrends, H. Wagner, A. Studer, O. Niehaus, R. Pöttgen, H. Eckert, F. Behrends, H. Wagner, A. Studer, O. Niehaus, R. Pöttgen, H. Eckert, Polynitroxides from alkoxyamine monomers: structural and kinetic investigations by solid state NMR, Macromolecules 46 (2013) 2553–2561, https://doi.org/10.1021/ma400351q.

[39] F. Wang, M.Z. Rong, M.Q. Zhang, Reversibility of solid state radical reactions in thermally remendable polymers with C-ON bonds, J. Mater. Chem. 22 (2012) 13076, https://doi.org/10.1039/c2jm30578j.

[40] J. Chen, J. He, Y. Tao, C. Li, Y. Yang, Synthesis of thermosensitive gel by living free radical polymerization mediated by an alkoxyamine inimer, Polymer (Guildf) 51 (2010) 4769–4775, https://doi.org/10.1016/j.polymer.2010.08.044.

[41] A. Aqil, A. Vlad, M. Piedboeuf, M. Aqil, N. Job, S. Melinte, C. Detrembleur, J. Christine, A new design of organic radical batteries (ORBs): carbon nanotube buckypaper electrode functionalized by electrografting †, (2015) 9301–9304. https ://doi.org/10.1039/c5cc02420j.

[42] M. Aqil, A. Aqil, F. Ouhib, A. El Idrissi, C. Detrembleur, C. Jérôme, RAFT polymerization of an alkoxyamine bearing acrylate, towards a well-defined redox active polyacrylate, RSC Adv. 5 (2015) 85035–85038, https://doi.org/10.1039/ C5RA16839B.

[43] M. Aqil, A. Aqil, F. Ouahib, C. Detrembleur, C. Jérôme, A. El Idrissi, A novel synthetic route toward a PTA as active materials for organic radical batteries, in: 2016 Int. Renew. Sustain. Energy Conf., IEEE, 2016: pp. 961–965. https://doi. org/10.1109/IRSEC.2016.7984033.

[44] D. Cordella, F. Ouhib, A. Aqil, T. Defize, C. Jérôme, A. Serghei, E. Drockenmuller, K. Aissou, D. Taton, C. Detrembleur, Fluorinated poly(ionic liquid) diblock copolymers obtained by cobalt-mediated radical polymerization-induced self- assembly, ACS Macro Lett. 6 (2017) 121–126, https://doi.org/10.1021/ acsmacrolett.6b00899.

[45] N. Patil, M. Aqil, A. Aqil, F. Ouhib, R. Marcilla, A. Minoia, R. Lazzaroni, C. Jérôme, C. Detrembleur, Integration of redox-active catechol pendants into poly(ionic liquid) for the design of high-performance lithium-ion battery cathodes, Chem. Mater. 30 (2018) 5831–5835, https://doi.org/10.1021/acs.chemmater.8b02307.

[46] N. Patil, D. Cordella, A. Debuigne, S. Admassie, C. Je, C. Detrembleur, A. Aqil, A. Debuigne, S. Admassie, C. Jérôme, C. Detrembleur, Surface- and redox-active multifunctional polyphenol-derived poly(ionic liquid)s: controlled synthesis and characterization, Macromolecules 49 (2016) 7676–7691, https://doi.org/ 10.1021/acs.macromol.6b01857.

[47] X. Chen, J. Zhao, J. Zhang, L. Qiu, D. Xu, H. Zhang, X. Han, B. Sun, G. Fu, Y. Zhang, F. Yan, Bis-imidazolium based poly(ionic liquid) electrolytes for quasi-solid-state dye-sensitized solar cells, J. Mater. Chem. 22 (2012) 18018, https://doi.org/ 10.1039/c2jm33273f.

[48] K. Kalaga, M.-T.F. Rodrigues, H. Gullapalli, G. Babu, L.M.R. Arava, P.M. Ajayan, Quasi-solid electrolytes for high temperature lithium ion batteries, ACS Appl. Mater. Interfaces 7 (2015) 25777–25783, https://doi.org/10.1021/ acsami.5b07636.

[49] A.F. Bratton, S.-S. Kim, C.J. Ellison, K.M. Miller, Thermomechanical and conductive properties of thiol-ene poly(ionic liquid) networks containing backbone and pendant imidazolium groups, Ind. Eng. Chem. Res. 57 (2018) 16526–16536, https://doi.org/10.1021/acs.iecr.8b04720.

[50] B.A. Paren, R. Raghunathan, I.J. Knudson, J.L. Freyer, L.M. Campos, K.I. Winey, Impact of building block structure on ion transport in cyclopropenium-based polymerized ionic liquids, Polym. Chem. 10 (2019) 2832–2839, https://doi.org/ 10.1039/C9PY00396G.

[51] G.D. Smith, O. Borodin, L. Li, H. Kim, Q. Liu, J.E. Bara, D.L. Gin, R. Nobel, H. Miyashiro, A comparison of ether- and alkyl-derivatized imidazolium-based room-temperature ionic liquids: a molecular dynamics simulation study, Phys. Chem. Chem. Phys. 10 (2008) 6301, https://doi.org/10.1039/b808303g.

[52] A. Triolo, O. Russina, R. Caminiti, H. Shirota, H.Y. Lee, C.S. Santos, N.S. Murthy, E. W. Castner Jr, Y. Umebayashi, K.R. Seddon, Comparing intermediate range order for alkyl- vs. ether-substituted cations in ionic liquids, Chem. Commun. 48 (2012) 4959, https://doi.org/10.1039/c2cc31550e.

[53] J. Sun, G.M. Stone, N.P. Balsara, R.N. Zuckermann, Structure–conductivity relationship for peptoid-based PEO- mimetic polymer electrolytes, Macromolecules 45 (2012) 5151–5156, https://doi.org/10.1021/ma300775b.

[54] R. Bouchet, S. Maria, R. Meziane, A. Aboulaich, L. Lienafa, J.-P. Bonnet, T.N. T. Phan, D. Bertin, D. Gigmes, D. Devaux, R. Denoyel, M. Armand, Single-ion BAB triblock copolymers as highly efficient electrolytes for lithium-metal batteries, Nat. Mater. 12 (2013) 452–457, https://doi.org/10.1038/nmat3602.

[55] S. Muench, A. Wild, C. Friebe, B. Haupler, T. Janoschka, U.S. Schubert, Polymer- ¨ based organic batteries, Chem. Rev. 116 (2016) 9438–9484, https://doi.org/ 10.1021/acs.chemrev.6b00070.

[56] A. Vlad, N. Singh, J. Rolland, S. Melinte, P.M. Ajayan, J.-F. Gohy, Hybrid supercapacitor-battery materials for fast electrochemical charge storage, Sci. Rep. 4 (2015) 4315, https://doi.org/10.1038/srep04315.

[57] G. Hernández, M. Işik, D. Mantione, A. Pendashteh, P. Navalpotro, D. Shanmukaraj, R. Marcilla, D. Mecerreyes, Redox-active poly(ionic liquid)s as active materials for energy storage applications, J. Mater. Chem. A 5 (2017) 16231–16240, https://doi.org/10.1039/C6TA10056B.